

Statistical Model for Polarization Mode Dispersion in Single Mode Fibers

*Hassan Abid Yasser**

Received 26, January, 2009

Acceptance 10, June, 2009

Abstract:

As the bit rate of fiber optic transmission systems is increased to more than 10 Gbps, the system will suffer from an important random phenomena, which is called polarization mode dispersion. This phenomenon contributes effectively to: increasing pulse width, power decreasing, time jittering, and shape distortion. The time jittering means that the pulse center will shift to left or right. So that, time jittering leads to interference between neighboring pulses. On the other hand, increasing bit period will prevent the possibility of sending high rates.

In this paper, an accurate mathematical analysis to increase the rates of transmission, which contain all physical random variables that contribute to determine the transmission rates, is presented. Thereafter, new mathematical expressions for: pulse power, peak power, time jittering, pulse width, and power penalty are derived. On the basis of these formulas, one can choose a certain operating values to reduce or prevent the effects of polarization mode dispersion.

Key words: PMD, statistics, SOP, PSP, Jones & Stokes spaces, transmission.

Introduction:

Polarization mode dispersion (PMD) arises in single mode fiber and fiber optic components due to a small difference in refractive index (birefringence) for a particular pair of orthogonal polarization states [1,2]. This index difference results in a difference in the propagation time called differential group delay (DGD) for waves traveling in these two polarization modes [3]. The propagation of a pulse through a long fiber can be very complicated since the birefringence varies randomly along the fiber. However, there are two special orthogonal polarization states, called principal states of polarization (PSP's), at the fiber input for which the output pulse is undistorted to first order, in spite of random changes in fiber birefringence [4,5]. An optical pulse polarized along a PSP does not split into two parts and maintains its

shape. In practice, the launched pulses are rarely polarized along one of PSP's, each pulse then splits into two parts that are delayed with respect to each other by a random amount [6,7].

This kind of PMD is commonly known as first-order PMD. Under first-order PMD, a pulse at the input of a fiber can be decomposed into two pulses with orthogonal states of polarization (SOP). Both pulses will arrive at the output of the fiber undistorted and polarized along different SOP's, the output SOP's being orthogonal [8,9]. Both the PSP's and the DGD are assumed to be frequency independent when only first-order PMD is being considered [10]. Second-order PMD effects account for the frequency dependence of the DGD and the PSP's. The frequency dependence of the DGD introduces an effective chromatic dispersion of

*Thi-Qar University, Science College

opposite sign on the signals polarized along the output PSP's [11]. PMD induced pulse broadening can move bits outside of their allocated time slots, resulting in errors and system failure in an unpredictable manner [1,5].

When the signal channel bit rates reached beyond 10 Gb/s, PMD became interesting to a larger technical community. PMD is now regarded as a major limitation in optical transmission systems in general, and an ultimate limitation for ultra-high speed signal channel systems based on standard single mode fibers [7,12]. PMD arises in optical fibers when the cylindrical symmetry is broken due to noncircular symmetric stress. The loss of such symmetry destroys the degeneracy of the two eigen-polarization modes in fiber, which will cause different group velocity dispersion parameters for these modes. In standard single mode fibers, PMD is random, i.e. it varies from fiber to fiber. Moreover, in the same fiber PMD will vary randomly with respect to wavelength and ambient temperature [6].

Disorder in single mode fibers arises in many different ways and has a negative effect. For example, amplifier noise[9], and random fiber birefringence (PMD)[8] that lead to random shifts in the pulse position (timing jitter), pulse broadening, and so to cause inter-symbol interference (ISI) impairment of a single digital transmission channel. The ISI impairment is caused by the DGD, $\Delta\tau$, between the two pulses propagating in the fiber when the input polarization of the signal does not match one of the PSP's of the fiber PMD impairments due to inter-channel effects that occur in polarization-multiplexed transmission systems. However, all PMD effects eventually cause destruction of bit patterns and lead to an increase of bit error rate, the most

important parameter describing performance in fiber communications systems [8,10]. The description of data stream degradation requires the use of statistical methods and opens a new field that may be called statistical physics of fiber-optic communication.

Our objective in this paper, is to model the PMD (at first order in w) density distribution and determined the probability of DGD that exceeds a particular value. Initially, the treatment will be quite general, involving standard equations for impulse response and density distribution of PMD. This general treatment will make it possible to estimate the density distribution of impulse response and power penalty. We will then consider the effect of all random variables on the output pulse. Due to the difficulty of the mathematical analysis, assuming the pulses are Gaussian form. The parameters that maximize density distributions of PMD, impulse response, and power penalty are determined. We proposed that the time jittering and pulse broadening effects may be reduced to minimum values by controlling on the angle between the PMD and input SOP vectors.

Theory

The effects of PMD are usually treated by means of the three-dimensional PMD vector that is defined as $\vec{\tau} = \tau_{pmd} \hat{p}$, where \hat{p} is a unit vector pointing in the direction of slow PSP, and τ_{pmd} is the DGD between the fast and slow components which is defined as [4]

$$\tau_{pmd} = |\vec{\tau}| = \sqrt{\tau_1^2 + \tau_2^2 + \tau_3^2} \quad \dots (1)$$

The PMD vector $\vec{\tau}$ gives in Stokes space the relation between the output SOP, \hat{s} , and the frequency derivative of the output SOP: $d\hat{s}(w)/dw = \vec{\tau}(w) \times \hat{s}(w)$. The PSP's are defined as the states that

$\bar{\tau}(w) \times \hat{s}(w) = 0$, so that no changes in output polarization can be observed close to these states at first order in w . To the first order, the impulse response of an optical fiber with PMD is defined as [7]

$$h_{pmd}(t) = \gamma_+ \delta(t - \tau_{pmd}/2) + \gamma_- \delta(t + \tau_{pmd}/2) \dots(2)$$

where γ_{\pm} are the splitting ratios. The factors γ_{\pm} and τ_{pmd} vary depending on the particular fiber and its associated stresses, where the splitting ratios can range from zero to one. Note that, the function $h_{pmd}(t)$ is normalized in the range $(-\infty$ to $\infty)$.

1 Splitting Ratios

For compactness in notations, the Jones vectors are written in the form $|p_+ \rangle$, $|p_- \rangle$, and $|s \rangle$, to distinguish them from the corresponding Stokes vectors $+\hat{p}$, $-\hat{p}$, and \hat{s} . Any Stokes vector \hat{a} is related to another one $|a \rangle$ in Jones space as $\hat{a} = \langle a | \vec{\sigma} | a \rangle$, where $\langle a |$ is the conjugate transpose of $|a \rangle$ and $\vec{\sigma} = (\sigma_1, \sigma_2, \sigma_3)$ is the Pauli spin vector, which is their components are defined as [8]

$$\sigma_1 = \begin{bmatrix} 1 & 0 \\ 0 & -1 \end{bmatrix}, \sigma_2 = \begin{bmatrix} 0 & 1 \\ 1 & 0 \end{bmatrix}, \sigma_3 = \begin{bmatrix} 0 & -i \\ i & 0 \end{bmatrix} \dots(3)$$

It is important to note that the angle between \hat{p} and \hat{s} in Stokes vector is θ , while the angle between $|p \rangle$ and $|s \rangle$ in Jones space is $\theta/2$. That is; if two vectors are perpendicular in Jones space then the corresponding two vectors in Stokes space are antiparallel.

Consider that the PSP's occur with a uniform distribution over the Poincare sphere, and that \hat{s} is aligned with the north pole of the sphere as shown in Fig.(1). The probability density of PSP's being in the range $d\theta$ about the angle θ relative to \hat{s} is proportional to the differential area

$2\pi \sin \theta d\theta$ sketched in the figure. As there is north/south symmetry in the differential area, the ranges $(0$ to $\pi/2)$ and $(\pi/2$ to $\pi)$ of θ are combined to obtain the combined probability density

$$p_{\theta}(\theta) = \sin \theta \dots(4)$$

For the effective range $(0$ to $\pi/2)$ describing the occurrence of PSP's with angle θ (and $\pi - \theta$) relative to $\pm \hat{s}$. The distribution $p_{\theta}(\theta)$ is properly normalized through the range 0 to $\pi/2$.

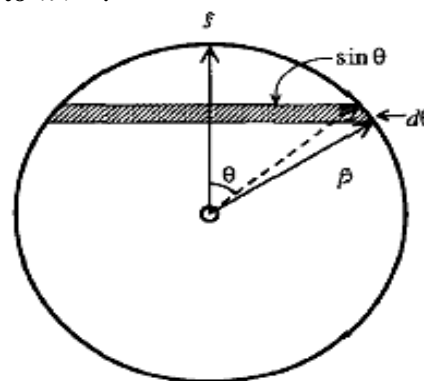


Fig.(1): Sketch of differential area on Poincare sphere as a function of elevation angle θ [5].

The analyses of splitting ratios have led to a number of advances important from fundamental as well as the technical point of view. The splitting ratios γ_{\pm} can be determined from the polarization vectors. In other words γ_{\pm} represent the projection of $|p_+ \rangle$ and $|p_- \rangle$ onto $|s \rangle$. Formally, $\gamma_{\pm} = |\langle s | p_{\pm} \rangle|^2$, where $|s \rangle$, $|p_+ \rangle$, and $|p_- \rangle$ are the input SOP and the two PSP's vectors. If the PSP's are defined as $|p_{\pm} \rangle = [p_{\pm x} \ p_{\pm y}]^t$, where t is the matrix transpose, then we can write $\langle p_{\pm} | p_{\pm} \rangle = \begin{bmatrix} p_{\pm x} \\ p_{\pm y} \end{bmatrix} \begin{bmatrix} p_{\pm x}^* & p_{\pm y}^* \end{bmatrix} = \begin{bmatrix} |p_{\pm x}|^2 & p_{\pm x} p_{\pm y}^* \\ p_{\pm y} p_{\pm x}^* & |p_{\pm y}|^2 \end{bmatrix} \dots(5)$ where $\langle p_{\pm} |$ are the transpose conjugate of $|p_{\pm} \rangle$. Now, it is straightforward to show that

$$\pm \hat{p} = \langle p_{\pm} | \vec{\sigma} | p_{\pm} \rangle = \begin{bmatrix} \pm p_1 \\ \pm p_2 \\ \pm p_3 \end{bmatrix} = \begin{bmatrix} \langle p_{\pm} | \sigma_1 | p_{\pm} \rangle \\ \langle p_{\pm} | \sigma_2 | p_{\pm} \rangle \\ \langle p_{\pm} | \sigma_3 | p_{\pm} \rangle \end{bmatrix} = \begin{bmatrix} |p_{\pm x}|^2 - |p_{\pm y}|^2 \\ p_{\pm x} p_{\pm y}^* + p_{\pm y} p_{\pm x}^* \\ i(p_{\pm y} p_{\pm x}^* - p_{\pm x} p_{\pm y}^*) \end{bmatrix} \dots (6)$$

Comparing Eqs.(4) and (5), we can extract

$$|p_{\pm} \rangle \langle p_{\pm}| = \frac{I_2 \pm \hat{p} \cdot \vec{\sigma}}{2} \dots (7)$$

$$\gamma_+ = \langle s | p_+ \rangle \langle p_+ | s \rangle = \frac{1}{2} \langle s | (I_2 + \hat{p} \cdot \vec{\sigma}) | s \rangle = \frac{1 + \hat{p} \cdot \hat{s}}{2} = \cos^2 \frac{\theta}{2} \dots (8 a)$$

$$\gamma_- = \langle s | p_- \rangle \langle p_- | s \rangle = \frac{1}{2} \langle s | (I_2 - \hat{p} \cdot \vec{\sigma}) | s \rangle = \frac{1 - \hat{p} \cdot \hat{s}}{2} = \sin^2 \frac{\theta}{2} \dots (8 b)$$

To this end, the relationship between the splitting ratios and elevation angle was calculated. Also, showing how the angle will be determined the values of γ_{\pm} that we have been calculated for this point.

2 Statistics of DGD

Throughout this subsection, the PMD statistics have been carefully analyzed that causes the variation in pulse properties. A proper measure of pulse width for pulses of arbitrary shapes is the root-mean square (rms) width of the pulse defined as $\tau_{rms} = \sqrt{\langle t^2 \rangle - \langle t \rangle^2}$. The PMD induced pulse broadening is characterized by the rms value of τ_{pmd} , τ_{rms} obtained after averaging over random birefringence changes. The second moment of τ_{pmd} is given by [6]

$$\langle \tau_{pmd}^2 \rangle = \tau_{rms}^2 = 2(\Delta\beta_1)^2 \ell_c^2 [L/\ell_c + e^{-L/\ell_c} - 1] \dots (9)$$

where ℓ_c is the correlation length that is defined as the length over which two polarization components remain correlated, $\Delta\beta_1 = v_{gx}^{-1} - v_{gy}^{-1}$ is related to the difference in group velocities along the two PSP's. For distances $L \gg 1km$, a reasonable estimate of pulse broadening was obtained by taking the limit $L \gg \ell_c$ in Eq.(9). The result is given by [7]

In turn, the splitting ratios can be calculated by using Eq.(6) and the fact that $\langle a | \hat{p} \cdot \vec{\sigma} | a \rangle = \hat{p} \cdot \hat{a}$

$$\tau_{rms} \approx \Delta\beta_1 \sqrt{2L\ell_c} = D_p \sqrt{L} \dots (10)$$

where D_p is known as the PMD parameter that takes the values (0.01–10) ps / \sqrt{km} . The variable τ_{pmd} has been determined to obey a Maxwellian distribution of the form [6]

$$p(\tau_{pmd}) = \sqrt{\frac{54}{\pi}} \frac{\tau_{pmd}^2}{\tau_{rms}^3} e^{-3\tau_{pmd}^2 / 2\tau_{rms}^2} \dots (11)$$

The mean of τ_{pmd} is done simply as follows

$$\bar{\tau}_{pmd} = \int_0^{\infty} \tau_{pmd} p(\tau_{pmd}) d\tau_{pmd} = \sqrt{\frac{8}{3\pi}} \tau_{rms} \dots (12)$$

Using Eq.(12), the Maxwellian distribution will take the form

$$p(\tau_{pmd}) = \frac{32}{\pi^2} \frac{\tau_{pmd}^2}{\bar{\tau}_{pmd}^3} e^{-4\tau_{pmd}^2 / \pi \bar{\tau}_{pmd}^2} \dots (13)$$

A cursory inspection of Eq.(13) reveals that the $p(\tau_{pmd})$ can be found if $\bar{\tau}_{pmd}$ is known. Here, a relationship for τ_{pmd} that will maximize $p(\tau_{pmd})$ can be found. The distribution $p(\tau_{pmd})$ has a maximum value at

$$\tau_{pmd} = \tau_{pmd}^{max} = \frac{\sqrt{\pi}}{2} \bar{\tau}_{pmd} \dots (14)$$

Eq.(14) provides a method for calculating the maximum likelihood value of τ_{pmd} if one knows $\bar{\tau}_{pmd}$.

Typically, if $\bar{\tau}_{pmd} = 2ps$ then $\tau_{pmd}^m = 1.77 ps$.

Using Eq.(13), the probability of τ_{pmd} exceeds a particular value can be found

$$P^{(1)} = \int_{\tau_{pmd}}^{\infty} p(\tau_{pmd}) d\tau_{pmd} = \frac{4}{\pi} x e^{-\frac{4}{\pi} x^2} + 1 - \operatorname{erf}\left(\frac{2}{\sqrt{\pi}} x\right) \dots (15)$$

where $x = \tau_{pmd} / \bar{\tau}_{pmd}$ and erf is the error function. For example, if the mean of DGD is $2 ps$, the probability for $\tau_{pmd} / \bar{\tau}_{pmd}$ exceeding 1 is 46% .

$$\tau_{eff} = \sqrt{\int_{-\infty}^{\infty} t^2 h_{pmd}(t) dt - \left[\int_{-\infty}^{\infty} t h_{pmd}(t) dt \right]^2} = \sqrt{\gamma_+ \gamma_-} \tau_{pmd} \dots (16)$$

The result may be simplified by substituting Eqs.(8) into (16) to yield

$$\tau_{eff} = \frac{1}{2} \sin \theta \tau_{pmd} \dots (17)$$

Using Eqs.(4) and (17), one can transform the density distribution for θ to the density for τ_{eff} as follows

$$p_{\tau_{eff}}(\tau_{eff}) = p_{\theta}(\theta(\tau_{eff})) \frac{d\theta}{d\tau_{eff}} = \frac{4\tau_{eff}}{\tau_{pmd} \sqrt{\tau_{pmd}^2 - 4\tau_{eff}^2}} \dots (18)$$

It is important to note that the probability density is a function of τ_{eff} and τ_{pmd} . As a consequence of this dependence, Eq.(18) can not be integrated to determine τ_{eff} because presence of the other variable τ_{pmd} . So, in the next, we seek about $p_{\tau_{eff}}(\tau_{eff})$ that is a function of τ_{eff} only to determine the statistical properties of output pulses.

The joint probability distribution $p(\tau_{eff}, \tau_{pmd})$ can be illustrated using Eqs.(13) and (18) as follows

$$p(\tau_{eff}, \tau_{pmd}) = \frac{64\tau_{eff}}{\pi \bar{\tau}_{pmd}^3} \frac{\tau_{pmd}}{\sqrt{\tau_{pmd}^2 - 4\tau_{eff}^2}} e^{-4\tau_{pmd}^2 / \pi \bar{\tau}_{pmd}^2} \dots (19)$$

Return to Eq.(17), it may be written as

$$\tau_{pmd} = \frac{2\tau_{eff}}{\sin \theta} . \text{ Since } 0 \leq \sin \theta \leq 1, \text{ such}$$

Expressed another way, if $\bar{\tau}_{pmd} = 2ps$ then 54 % of the time τ_{pmd} will be less than $2ps$.

3 Statistics of Impulse Response

The rms width of the impulse response, τ_{eff} , can be readily calculated by substituting Eq.(2) into $\tau_{rms} = \sqrt{\langle t^2 \rangle - \langle t \rangle^2}$ to yield

that $2\tau_{eff} \leq \tau_{pmd} < \infty$. The probability distribution $p(\tau_{eff})$ can be found by integrating Eq.(19) about τ_{pmd} through the range $2\tau_{eff} \leq \tau_{pmd} < \infty$ to obtain

$$p(\tau_{eff}) = \frac{32\tau_{eff}}{\pi \bar{\tau}_{pmd}^2} e^{-16\tau_{eff}^2 / \pi \bar{\tau}_{pmd}^2} \dots (20)$$

At a basic level, Eq.(18) is the same as Eq.(20) but the latter is a function of τ_{eff} only, which can be integrated to obtain τ_{eff} . However, both equations are normalized properly. The mean value of τ_{eff} can be determined as

$$\bar{\tau}_{eff} = \int_0^{\infty} \tau_{eff} p(\tau_{eff}) d\tau_{eff} = \sqrt{\frac{\pi}{24}} \tau_{rms} \dots (21)$$

So, Eq.(20) may be written as

$$p(\tau_{eff}) = \frac{\pi}{2} \frac{\tau_{eff}}{\bar{\tau}_{pmd}^2} e^{-\pi \tau_{eff}^2 / 4 \bar{\tau}_{pmd}^2} \dots (22)$$

The distribution $p(\tau_{eff})$ has a maximum value at

$$\tau_{eff}^{\max} = \tau_{eff}^{\max} = \sqrt{\frac{\pi}{32}} \bar{\tau}_{pmd} \dots (23)$$

This is equivalent to find the maximum likelihood value of τ_{eff} if one knows $\bar{\tau}_{pmd}$. Typically, if $\bar{\tau}_{pmd} = 2ps$ then $\tau_{eff}^{\max} = 0.63 ps$. Using Eq.(22), the probability of τ_{pmd} exceeds a particular value can be found

$$P^{(2)} = \int_{\tau_{eff}}^{\infty} p(\tau_{eff}) d\tau_{eff} = e^{-\pi \tau_{eff}^2 / 4 \bar{\tau}_{pmd}^2} \dots (24)$$

For example, if $\bar{\tau}_{pmd} = 2ps$, then $\bar{\tau}_{eff} = \pi\bar{\tau}_{pmd} / 8 = 0.79ps$ and the probability for $\tau_{eff} / \bar{\tau}_{eff}$ exceeding $1ps$ is 45%. That is, if $\bar{\tau}_{eff} = 0.79ps$ then τ_{pmd} will be less than $0.79ps$ at 55% of the time.

4 Power Penalty

In the first-order picture, PMD splits the input signal entering the fiber into two orthogonally polarized components that are delayed by τ_{pmd} relative to each other during transmission. The impairment caused by this effect can be expressed as a power penalty of the form [12]

$$\varepsilon(dB) = \frac{K}{4T^2} \tau_{pmd}^2 \sin^2 \theta = \frac{K}{T^2} \tau_{eff}^2 \dots (25)$$

where the penalty expressed in dB is assumed to be small, T is the bit interval, and K is a dimensionless parameter takes the value from 10 to 70 depend on pulse shape, modulation format, and specific receiver characteristics. It is straightforward to note that the penalty will minimize by decreasing DGD, increasing bit period, and making the elevation angle around $\theta = 0$ or $\theta = \pi$.

The mean penalty parameter can be determined using Eqs.(22) and (25) as follows

$$\bar{\varepsilon} = \int_0^\infty \varepsilon(\tau_{eff}) p(\tau_{eff}) d\tau_{eff} = \frac{\pi K}{16T^2} \bar{\tau}_{pmd}^2 \dots (26)$$

This allow us to easily transform the Rayleigh density, i.e. Eq.(22), of τ_{eff} to the density for ε and obtain the following distribution

$$p_\varepsilon(\varepsilon) = p_{\tau_{eff}}(\tau_{eff}(\varepsilon)) \frac{d\tau_{eff}}{d\varepsilon} = \frac{1}{\bar{\varepsilon}} e^{-\varepsilon/\bar{\varepsilon}} \dots (27)$$

Using this distribution, the probability of ε exceeding a particular value can be found as follows

$$P^{(3)} = \int_\varepsilon^\infty p_\varepsilon(\varepsilon) d\varepsilon = e^{-\varepsilon/\bar{\varepsilon}} \dots (28)$$

Typically, if $\bar{\tau}_{pmd} = 2ps$, $K = 30$, and $T = 20ps$, then $\bar{\varepsilon} = 0.059dB$ and the probability for $\varepsilon/\bar{\varepsilon}$ exceeding 1 is 37%. That is, if $\bar{\varepsilon} = 0.059dB$, then ε will be less than $0.059dB$ at 63% of the time.

We are particularly interested in the relations of τ_{pmd}^{max} to find τ_{eff}^{max} and then the maximum likelihood penalty ε^{max} . That is; the maximum likelihood τ_{pmd} will determine the maximum likelihood τ_{eff} . As a consequence, the maximum likelihood penalty will be calculated. All variables τ_{pmd}^{max} , τ_{eff}^{max} , and ε^{max} are depended on the parameters D_p and \sqrt{L} . For illustration, the density distributions of τ_{pmd} , τ_{eff} , and ε are computed in Fig.(2).

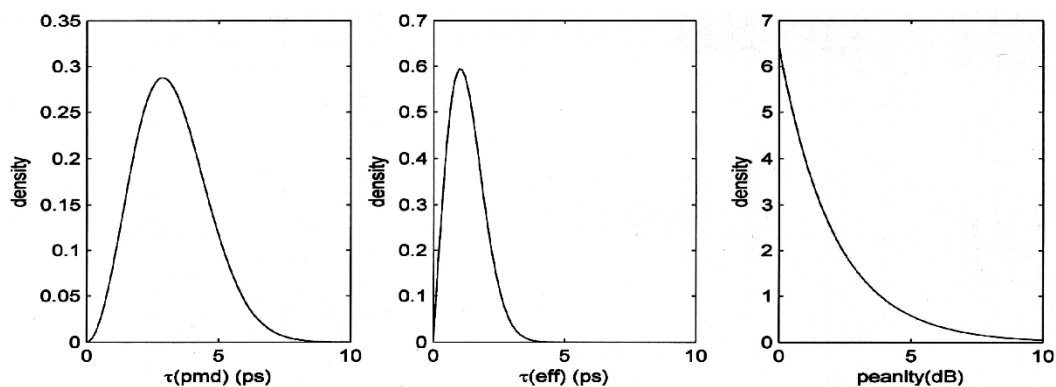


Fig.(2): density distributions $p(\tau_{pmd})$, $p(\tau_{eff})$, and $p(\varepsilon)$.

2.5 Pulse Characteristics

Using the PSP's as an orthogonal basis set, any input or output polarization can be expressed as the vector sum of two components,

$$|E_{out}(t)\rangle = \gamma_+ E_{in}(t - \tau_{pmd}/2) |p_+\rangle + \gamma_- E_{in}(t + \tau_{pmd}/2) |p_-\rangle \dots (29)$$

where $E_{in}(t)$ is the input electric field.

Before finding the output power $P_{out}(t) = \langle E_{out}(t) | E_{out}(t) \rangle$, it is important to point out orthogonality properties of Jones vectors, that is; $\langle p_\pm | p_\mp \rangle = 0$ and $\langle p_\pm | p_\pm \rangle = 1$. Note that, we perform derivation using a normalized Gaussian pulse that takes the form $E_{in}(t) = \exp(-t^2/2t_0^2)$. Therefore, according to Eq.(29), the shifted pulses will reshape as

each aligned with a PSP. Within the realm of the first-order PMD, the output electric field from a fiber with PMD has the form [9]

$$E_{in}(t - \tau_{pmd}/2) = \exp\left[-\frac{(t - \tau_{pmd}/2)^2}{2t_0^2}\right] \dots (30 a)$$

$$E_{in}(t + \tau_{pmd}/2) = \exp\left[-\frac{(t + \tau_{pmd}/2)^2}{2t_0^2}\right] \dots (30 b)$$

where t_0 is the initial pulse width.

Substituting Eqs.(8) and (30) into (29), using the output power definition, using the orthogonality properties of Jones vectors, and simplified the result, we obtain the following expression

$$P_{out}(t) = \left[\cos^2(\theta/2) e^{-t\tau_{pmd}/2t_0^2} + \sin^2(\theta/2) e^{t\tau_{pmd}/2t_0^2} \right] e^{-(4t^2 + \tau_{pmd}^2)/4t_0^2} \dots (31)$$

The width of the output pulse t_1 can be determined using Eq.(31) as follows

$$t_1 = \sqrt{\int_{-\infty}^{\infty} t^2 P_{out}(t) dt - \left[\int_{-\infty}^{\infty} t P_{out}(t) dt \right]^2} = \sqrt{t_0^2 + (\tau_{pmd}/2) \sin^2 \theta} \dots (32)$$

The time jittering of the pulse can be found by determining the maximum value of $P_{out}(t)$. This maximum value will happen at

$$t = t_{peak} = \frac{\tau_{pmd}}{2} \cos \theta \dots (33)$$

$$P_{peak}(\tau_{pmd}, \theta) = \cos^2(\theta/2) e^{-\sin^2(\theta/2) \tau_{pmd}^2 / t_0^2} + \sin^2(\theta/2) e^{-\cos^2(\theta/2) \tau_{pmd}^2 / t_0^2} \dots (34)$$

At this point, we drive a formulas for the output power form, final width, time jittering (shifting), and peak power as functions of the random physical variables θ and τ_{pmd} . Eqs.(31-34) are considered as the main achievement of this work.

6 Special cases

Now, using Eqs.(31) to (34), very important special cases may be illustrated

1. For $\theta = random$, $\tau_{pmd} = 0$ (SOP enters with random angle, no PMD)

$$P_{out}(t) = e^{-t^2/t_0^2} = P_{in}(t), \quad t_1 = t_0, \quad t_{peak} = 0, \quad P_{peak} = 1, \quad \varepsilon = 0$$

The peak power, as a function of DGD and an angle θ , at the pulse center can be determined by substituting Eq.(33) into Eq.(31) as follows

Note that, this case does not represented any physical fact but it introduced for illustration only.

2. For $\theta = 0$, $\tau_{pmd} = random$ (SOP parallels to PMD vector, random PMD value)

$$P_{out}(t) = e^{-(t - \tau_{pmd}/2)^2 / t_0^2}, \quad t_1 = t_0, \quad t_{peak} = \tau_{pmd}/2, \quad P_{peak} = 1, \quad \varepsilon = 0$$

3. For $\theta = \pi$, $\tau_{pmd} = random$ (SOP anti-parallel to PMD, random PMD value)

$$P_{out}(t) = e^{-(t + \tau_{pmd}/2)^2 / t_0^2}, \quad t_1 = t_0, \quad t_{peak} = -\tau_{pmd}/2, \quad P_{peak} = 1, \quad \varepsilon = 0$$

4. For $\theta = \pi/2$, $\tau_{pmd} = random$ (SOP and PMD vectors are orthogonal, random PMD value)

$$P_{out}(t) = \cosh\left[\frac{t\tau_{pmd}}{2t_0^2}\right] e^{-(4t^2 + \tau_{pmd}^2)/4t_0^2}, \quad t_1 = \sqrt{t_0^2 + (\tau_{pmd}/2)^2}$$

$$t_{peak} = 0, \quad P_{peak} = e^{-\tau_{pmd}^2/2t_0^2}, \quad \varepsilon = K\tau_{pmd}^2/4T^2$$

Determination of power formula, pulse width, time jittering, and penalty at an angles $\theta = 0, \pi$ is very easy as well as whether the case $\tau_{pmd} = 0$, while the calculation at $\theta = \pi/2$ has some difficulty. Note that, the fourth special case is presented as an example, but in fact all angles other than $\theta = 0, \pi$ will make some mathematical difficulty. All details will shown at simulation results section. The power formula at $\theta = \pi/2$ consists of a multiplication of three terms which are: $\cosh(t\tau_{pmd}/2t_0^2)$, e^{-t^2/t_0^2} , and $e^{-\tau_{pmd}^2/4t_0^2}$. Plotting the pulse shape depends on t , so the shape is affected by $\cosh(t\tau_{pmd}/2t_0^2)$ and e^{-t^2/t_0^2} only, but the term $e^{-\tau_{pmd}^2/4t_0^2}$ does not affected by τ_{pmd} . The term $\cosh(t\tau_{pmd}/2t_0^2)$ is an even function of t , increasing τ_{pmd} does not changed the shape of $\cosh(t\tau_{pmd}/2t_0^2)$ significantly but will make the pulse curve to raise more on both sides of $t = 0$. For $\tau_{pmd} \geq t_0$, the term $\cosh(t\tau_{pmd}/2t_0^2)$ will lead to make a symmetric two lobes around $t = 0$ at the points

$$t = -\sin^2(\theta/2)(\tau_{pmd}/t_0)^2$$

$$t = \cos^2(\theta/2)(\tau_{pmd}/t_0)^2$$

For all other angles, except $\theta = 0, \pi/2, \pi$, the two lobes are not symmetric. Thereafter, at $\theta = 0, \pi$, the lobes will not appear. In other words, all angles except $\theta = 0, \pi/2, \pi$, will

distort the pulse shape. The stronger distortion is happen at $\theta = \pi/2$.

Results and Discussion:

The parameters used in the simulation are as follows: $L = 50 km$, $D_p = 0.5 ps/\sqrt{km}$, $K = 30$, $t_0 = 5 ps$, and $T = 20 ps$. The bit period is selected to be $T = 20 ps$ to prevent any interference between neighborhood signals that represent distinct bits. Fig.(3) represents the pulses shape, where the solid line is the original pulse, while the discrete lines are the resulted pulses with different values of τ_{pmd} ranging from 0 to 8ps, where the closest to $t = 0$ is the pulse that has least value of τ_{pmd} . Fig.(4) represents pulse width, time jittering (shifting), peak power, and penalty as functions of τ_{pmd} and θ . At the angle $\theta = 0$, one note that the pulse is faced only by a displacement to right at $t_{peak} = \tau_{pmd}/2$. By rising θ , the pulse width and distortion will increase, while the power and shifting will decrease. These variations are greatest at $\theta = \pi/2$. After $\theta = \pi/2$, the effects are reversed. At $\theta = \pi$, again the pulse is faced only by a displacement but to left at $t_{peak} = -\tau_{pmd}/2$. It is clear from Fig.(4) that the penalty could be greater if $\theta = \pi/2$ and will be zero at $\theta = 0$ or π .

Depending on the above discussion, we can illustrate the following: the input pulse with SOP that matches one of the PSP's will not suffer any effects except displacement at $t_{peak} = \pm\tau_{pmd}/2$, while the pulse that enters the fiber with an angle $\theta = \pi/2$ will face a greatest variations but without time jittering. According to the values used in the simulation, $\bar{\tau}_{pmd} = 3.26ps$, $\tau_{pmd}^{max} = 1.28ps$,

$\tau_{eff}^{max} = 1.02ps$, and $\varepsilon^{max} = 0.07dB$. In other words, the most frequent of τ_{pmd} is $\tau_{pmd}^{max} = 1.28ps$, and the most frequent of τ_{eff} is $\tau_{eff}^{max} = 1.02ps$. Consequently, seeing from Figs.(3) and (4), the changing in pulse shape, width, and time jittering are insignificant, especially at $\theta = 0$ or π . Also, can note that, the most frequent penalty is $\varepsilon^{max} = 0.07dB$, which is very small and does not effect system properties.

We can not fail to mention that the increasing of PMD parameter and fiber length will lead to increase the values above and thus adversely affecting the functioning of the system specifications. Finally, the angle θ can control an important factors that are affecting all physical properties of the system, where the best values are $\theta = 0, \pi$. Table(1) summarizes all cases of Figs.(3) and (4).

Table (1): pulse properties with different values of θ and τ_{pmd} .

τ_{pmd}	θ	shape distortion	pulse broadening	time jittering	peak value	power penalty
random	0	No	No	right	1	No
random	$\pi/8$	Yes	Yes	right	< 1	Yes
random	$2\pi/8$	Yes	Yes	right	< 1	Yes
random	$3\pi/8$	Yes	Yes	right	< 1	Yes
random	$\pi/4$	Yes maximum	Yes maximum	No	< 1 minimum	Yes maximum
random	$5\pi/8$	Yes	Yes	left	< 1	Yes
random	$6\pi/8$	Yes	Yes	left	< 1	Yes
random	$7\pi/8$	Yes	Yes	left	< 1	Yes
random	π	No	No	left	1	No
$\tau_{pmd} = 0$	random	No	No	No	1	No

Conclusions:

Identifying the most frequent value τ_{pmd}^{max} leads to identify all other random variables: τ_{eff}^{max} , ε , t_1 , P_{peak} , and t_{peak} . As a consequence, the extent distortions that are faced the pulse may be determined. It is important to note that, the system properties did not change with τ_{pmd} , but will change with the most frequent value τ_{pmd}^{max} . Therefore, the system will work at most its time with values that are calculated in results section. At very

small time, the system will use another values, which are different from the best values $\bar{\tau}_{pmd} = 3.26ps$, $\tau_{pmd}^{max} = 1.28ps$, $\tau_{eff}^{max} = 1.02ps$, $\varepsilon^{max} = 0.07dB$, and $\tau_{pmd}^{max} = 1.28ps$. In other words, the most frequent of τ_{pmd} is, and the most frequent of τ_{eff} is $\tau_{eff}^{max} = 1.02ps$. Generally, reducing PMD parameter, reducing fiber length, and preserving the angle values at $\theta = 0$ or π will make the system to achieve the desired objectives.

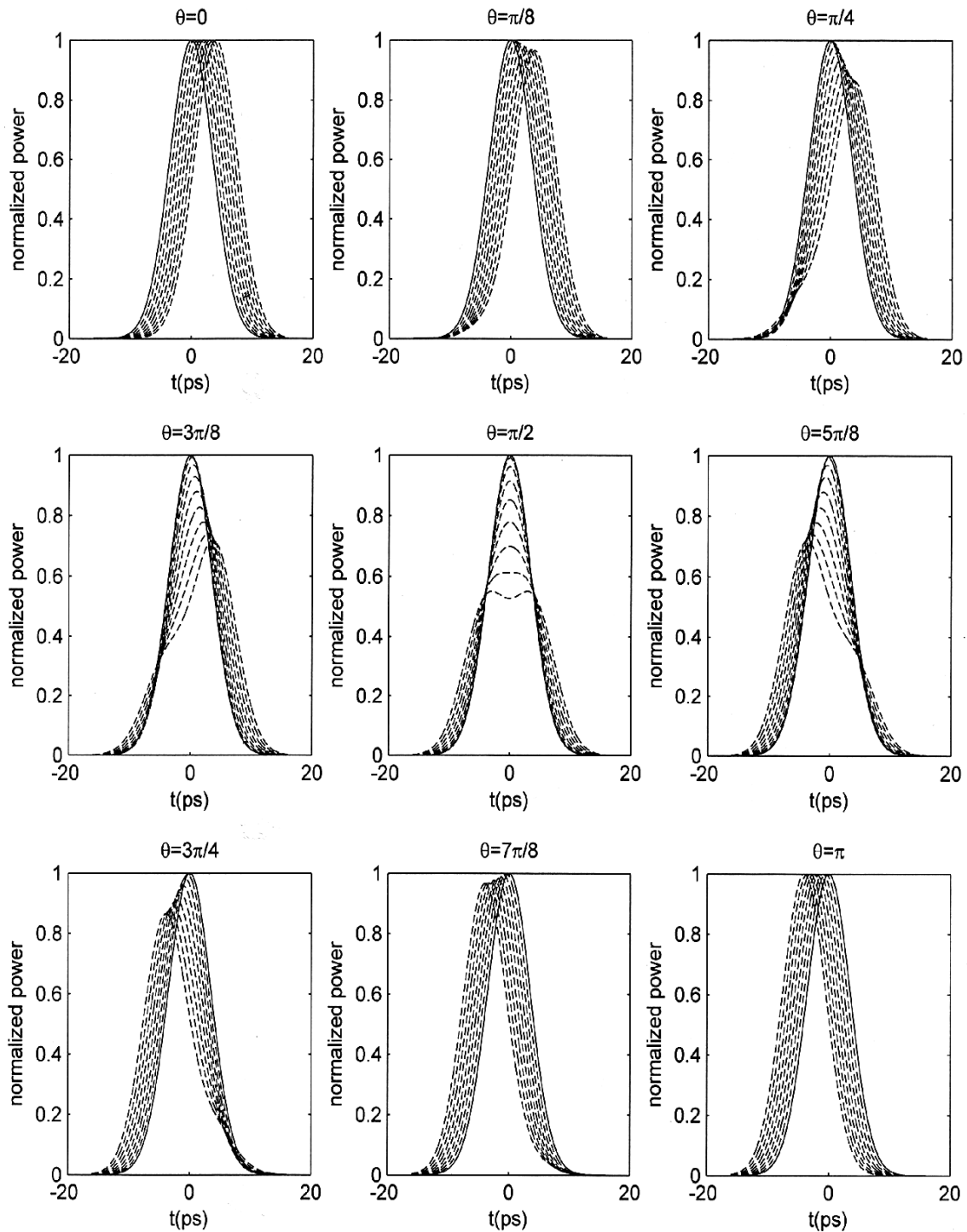


Fig.(3): pulse shape with different value of τ_{pmd} and θ , the solid line represents the original pulse while the discrete lines represent the resulted pulses for different values of τ_{pmd} , where the lower value of τ_{pmd} is the closest to the pulse center.

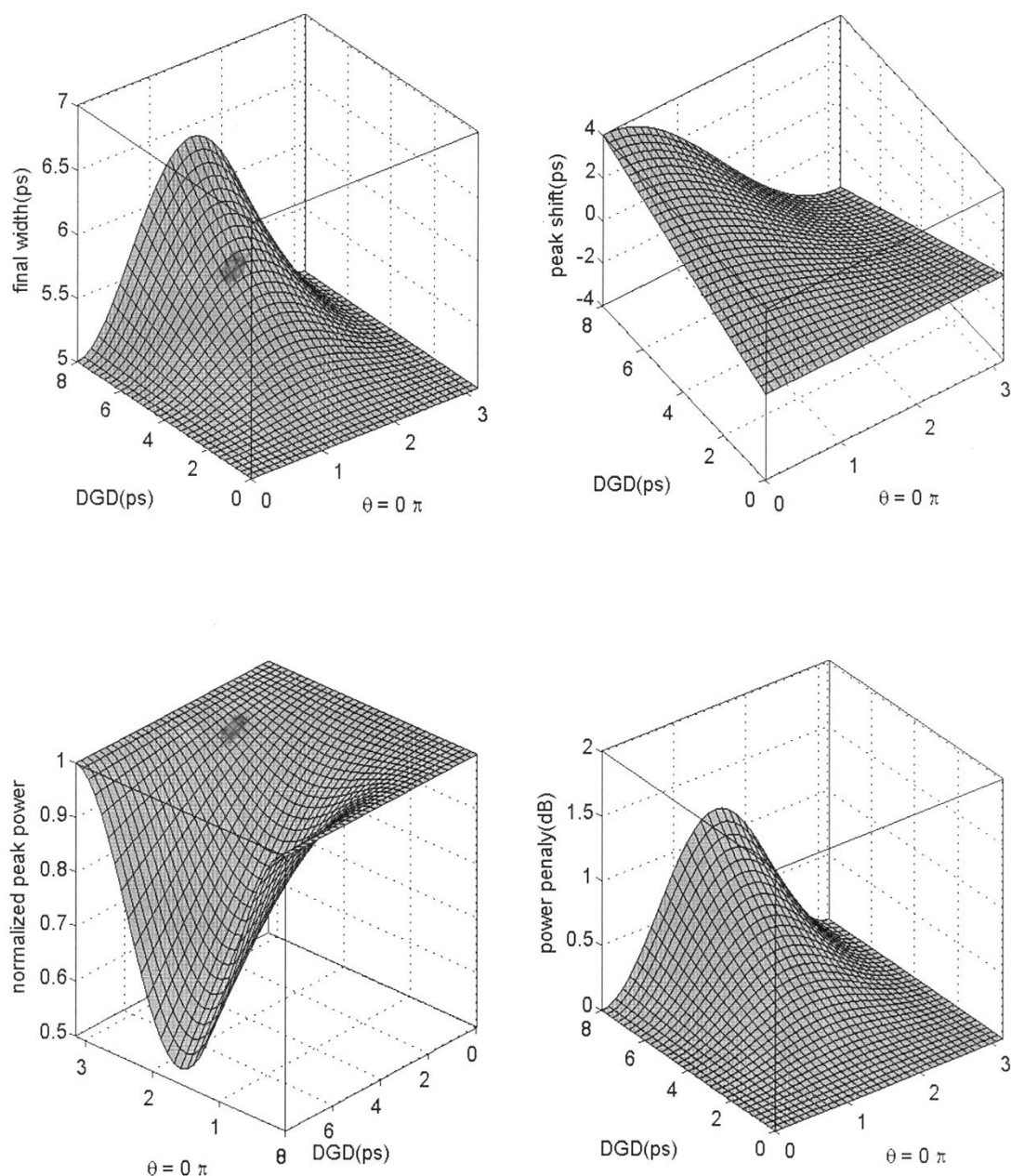


Fig.(4): final width, peak shift, normalized peak power, and power penalty as a function of DGD and angle θ .

References:

1. Karlsson M., 1994, "Polarization Mode Dispersion Induced Pulse Broadening in Optical Fibers", *Optics Lett.* 23: 688-690.
2. Elbers J., Glingener C., Duser M., and Voges E., 1997, "Modeling of Polarization Mode Dispersion in Single Mode Fibers", *Elect. Lett.* 33(22): 662-664.
3. McCurdy A., Sengupta A., and Glodis P., 2004, "Compact Measurement of Low PMD Optical Telecommunication Fibers", *Optics Express* 12(6):1109-1118.
4. Wang D. and Menyuk C.R., 2001, "Calculation of Penalties Due to Polarization Effects in Long-Haul WDM System Using a Stokes Parameter Mode", *J. Lightwave Tech* 19(4): 487-494.
5. Agrawal G. P., 2005, "Lightwave Technology: Telecommunication

- Systems", 1st Edition, Wiley Interscience.
6. Foshchini G. and Poole C., 1991, "Statistical Theory of Polarization Dispersion in Single Mode Fibers", J. Lightwave Tech. 9: 1439-1456.
 7. Agrawal G. P., 2002, "Fiber-Optic Communication Systems", 3rd Edition, Wiley Interscience.
 8. Gordon J. and Kogelnik H., 2000, "PMD Fundamentals: Polarization Mode Dispersion in Optical Fibers", Proc. Natl. Acad. Sci. 97(9): 4541-4550.
 9. Wang D. and Menyuk C.R., 2001, "Calculation of Penalties Due to Polarization Effects in Long-Haul WDM system Using a Stokes Parameter Mode", J. Lightwave Tech. 19(4): 487-494.
 10. Sunnerud H., Karlsson M., Xie C., and Andrekson P., 2002, "Polarization Mode Dispersion in High Speed Fiber Optic Transmission Systems", J. Lightwave Tech. 20(12): 2204-2219.
 11. Ibragimov E. and Shtengel G., 2002, "Statistical Correlation Between First and Second Order PMD", J. Lightwave Tech. 20(4): 586-590.
 12. Mahgerftech D. and Menyuk C. R., 1999, "Effects of First-Order PMD Compensation on the Statistics of Pulse Broadening in Fiber with Random Varying Birefringence", IEEE Photo. Tech. Lett. 13(3): 340-342.

نموذج إحصائي لتشتت نمط الاستقطاب في الألياف منفردة النمط

حسن عبد ياسر*

*جامعة ذي قار - كلية العلوم

الخلاصة:

عند زيادة نسبة الإرسال في الألياف البصرية إلى أكثر من 10 كيكابت/ثانية فإن النظام سوف يعاني من ظاهره عشوائية مهمة هي تشتت نمط الاستقطاب والتي تساهم بشكل فعال في زيادة عرض النبضة، نقصان قدرتها، إزاحة مركزها، وتشوه شكلها. أن إزاحة الموقع تعني احتمال حدوث تداخل بين النبضات المتجاورة، وإذا حددنا فترة البت بمقدار كبير فأن ذلك يعني عدم إمكانية تحقيق نسب إرسال عالية، لذلك يجب وضع صيغ رياضية دقيقة من أجل زيادة نسب الإرسال.

في هذا البحث، تم تحليل جميع المتغيرات الفيزيائية العشوائية التي تساهم في تحديد نسب الإرسال واستطعنا وضع صيغ رياضية جديدة لكل من: طاقة النبضة، طاقة القمة، ومقدار إزاحة القمة، عرض النبضة، والخسارة المتحققة. على أساس هذه الصيغ الرياضية يمكن اختيار قيم تشغيل معينة لتقليل أو منع تأثيرات تشتت نمط الاستقطاب.